Type of contribution:
Editorial
▶ Research Paper
Case Study
Review Paper
Scientific Data
Report of Tech. Application

mesi e-issn. 2798-5245

Mechanical Engineering for Society and Industry
Vol. 4, No. 1 (2024) pp 50-67
https://doi.org/10.31603/mesi.10996

Heat transfer performance of Al_2O_3-TiO_2-SiO_2 ternary nanofluids in plain tube with wire coil inserts

Anwar Ilmar Ramadhan[1]*, **Wan Hamzah Azmi**[2], **Efrizon Umar**[3], **Alvika Meta Sari**[4]

[1] Department of Mechanical Engineering, Universitas Muhammadiyah Jakarta, Jakarta 10510, **Indonesia**
[2] Faculty of Mechanical and Automotive Engineering Technology, Universiti Malaysia Pahang Al-Sultan Abdullah, 26600 Pekan, Pahang, **Malaysia**
[3] National Research and Innovation Agency, Jl. Tamansari No 71 Bandung, Bandung 40132, **Indonesia**
[4] Department of Chemical Engineering, Universitas Muhammadiyah Jakarta, Jakarta 10510, **Indonesia**
✉ anwar.ilmar@umj.ac.id

This article contributes to:
7 AFFORDABLE AND CLEAN ENERGY
SUSTAINABLE DEVELOPMENT GOALS

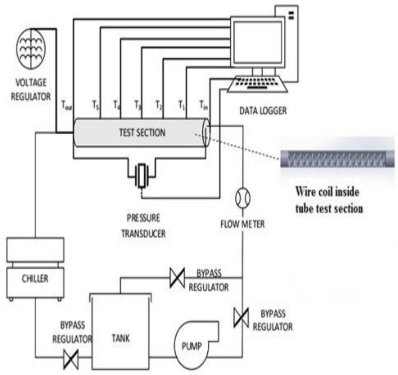

Highlights:

- This study investigates the heat transfer performance of Al2O3-TiO2-SiO2 ternary nanofluids in regular tubes with wire coil inserts.
- The highest increase in thermal conductivity of 24.8% was observed for the ternary nanofluid at a volume concentration of 3.0%, which also showed the highest viscosity at all temperatures.
- The maximum heat transfer increase in plain tubes with wire coil inserts (P/D-0.83) was achieved with a volume concentration of 3.0%.

Abstract

The ternary nanofluids are considered due to their advantages in overcoming the stability drawback of mono and binary nanofluids. This study aims to heat transfer performance of Al_2O_3-TiO_2-SiO_2 ternary nanofluids in plain tube with wire coil under experimental. The ternary nanofluids were formulated using the composition ratio of 20:16:64 by volume in various volume concentrations ranging from 0.5 to 3.0%. Thermal conductivity and dynamic viscosity of ternary nanofluids were measured with KD2 Pro Thermal Properties Analyzer and Brookfield LVDV III Rheometer. Experimental forced convection heat transfer was carried out using a fabricated setup for Reynolds numbers from 2,300 to 12,000 at bulk temperature of 70 °C in plain tubes with wire coil inserts ($0.83 \leq P/D \leq 2.50$). Experimental results are highest thermal conductivity enhancement of 24.8% was obtained for ternary nanofluids at 3.0% volume concentration. The 3.0% volume concentration also shows the highest viscosity at all temperatures. The maximum heat transfer improvement for ternary nanofluids in a plain tube with wire coil (*P/D*-0.83), was attained by 3.0% volume concentration of up to 199.23%. The average TPF of the wire coil increases compared to the plain tube and improves further with volume concentrations in the range of 2.39 to 2.84.

Keywords: Experimental; Heat transfer performance; Plain tube; Ternary nanofluids; Wire coil

Article info
Submitted: 2024-02-07
Revised: 2024-04-03
Accepted: 2024-04-25

Publisher
Universitas Muhammadiyah Magelang

1. Introduction

In recent years, nanofluids have attracted the attention of many researchers for various applications [1]–[9]. In general, hybrid nanofluids can be considered a new class of nanofluids that require more extensive research. According to the literature, hybrid nanofluids terminology can be divided into two major research topics, binary and ternary nanofluids. However, in the previous study, most researchers have used the term hybrid to refer to binary nanofluids [10]–[15]. Heat transfer is the principal utilisation of binary nanofluids due to their ability to impart the optimal qualities of most of their constituents. It is believed that binary nanofluids are an extension of mono nanofluids, in which the single base fluid contains two or more nanoparticles that are suspended or dispersed in the fluid [16]. Carbon nanotubes, also known as CNTs, are a component of hybrid materials that have found application in sensors, including electrochemical, nanocatalysts, and biosensors. Even so, there are still some limitations to how these nanomaterials can be used as binary nanofluids [17]. It has been revealed that the improved thermal conductivity of nanofluids is one of the most critical aspects in enhancing the performance of numerous heat transfer applications. Binary nanofluids have a significant increase in thermo-physical and heat transfer capabilities, allowing them to outperform conventional fluids and mono nanofluids in heat transfer applications [18]–[21].

Research on hybrid nanofluids by combining three different nanoparticles into base fluids called ternary nanofluids was initiated by Mousavi, et al. [22]. Ternary nanofluids are developed to improve the thermo-physical properties much more than existing mono and binary nanofluids [22]–[24]. Several researchers investigated the ternary nanofluids by looking at their ability to sustain better stability, characterization, and thermo-physical properties to evaluate the heat transfer capabilities for applications in thermal engineering systems [22], [25]–[29]. The ternary nanofluid preparation uses a composition of three nanoparticles originating from metal and metal oxide by dispersing into several base fluids. Mousavi, et al. [22] investigated the thermo-physical properties of ternary nanofluids by incorporating three metal oxide nanoparticles dispersed in a base of water. Their study aims to improve nanofluids' stability and increase their thermal properties. The ternary nanofluids with dissimilar base fluids will outperform at different stability behaviour and thermal properties enhancement [23]. Therefore, the ternary nanofluids' characteristics for heating and cooling must be studied extensively for application in thermal engineering systems. According to Muzaidi, et al. [30], the ternary nanofluids increased the heating speed of the solar thermal system. Thus, the concept of ternary nanofluids has become an exciting topic of interest for current and future research works [27], [31]–[34].

Previous research has examined the use of binary nanofluids in heat transfer applications, with several studies conducted by various researchers [18], [35]–[42]. In one of these studies, Baby and Ramaprabhu [42] looked at how well binary f-MWNT/f-HEG nanofluids mixed with water-based fluids transferred heat at different Reynolds numbers and volume concentrations. Their analysis was mainly about turbulent flow with a constant heat flux at the edges. The tested volume concentrations were 0.005% and 0.01%, and their Reynolds numbers were 4500, 8700, and 15,500. At a Reynolds number of 4500, the results showed that the heat transfer coefficient went up by 181% for volume concentrations of 0.005% and by 264% for concentrations of 0.01% at the entrance of the test section. At the end of the test section, heat transfer was improved by 166% and 206% for the same volume concentrations and Reynolds numbers. Also, the increase in heat transfer was more considerable at a high Reynolds number. This result was measured at both the beginning and end of the test sections. It is important to note that the heat transfer coefficient of EG-based fluids increased as volume concentrations and Reynolds numbers increased. This finding contrasts with the behaviour of water-based nanofluids, where heat transfer enhancement was observed to be greater at high Reynolds numbers. These results provide valuable guidelines for determining optimal volume concentrations of binary nanofluids in heat transfer applications.

Keklikcioglu and Ozceyhan [43] investigated the influence of wire coil on heat transmission and pressure loss in a tube. The setup with $P/D = 1$ yielded the best overall efficiency of augmentation. The Nusselt number and pressure drop decreased with the wire coil's separation from the tube wall. While this happened, Promvonge [44] provided experimental data for heat transmission and flow friction in a circular tube of square-sectioned wire coils. Several studies examined the heat transmission and frictional qualities of tubes with wire coil inserts and various nanofluid varieties as working fluids [19], [45]–[47]. The performance of the thermo-hydraulic system in a tube with a snail entry and wire coil insert was examined by Promvonge, et al. [48]. Saha [49] investigated the friction coefficient and heat transfer parameters of laminar oil flow in rectangular and square ducts with transverse ribs and wire coils. Feng, et al. [50] evaluated the performance of a rectangular microchannel heat sink (MCHS) with wire coil inserts regarding coupled laminar liquid flow and heat transmission.

Chougule, et al. [51] investigated the heat transmission and friction factor properties of MWCNT/water nanofluid flowing through a horizontally heated tube with and without a wire coil. The overall flow pattern and heat transfer enhancement in oscillatory-baffled reactors with helical coil inserts are investigated using numerical analysis. The increased heat transfer rate was addressed while the combined impact of oscillatory motion and helical coil inserts was considered [52]. A wire coil inserts in a circular tube was tested for its thermal performance in laminar and transitional flow fields by García, et al. [53]. It has been proven that heat transmission may be explored experimentally and numerically by placing a wire coil within the tube. These findings are supported by several previous works connected to the topic. Wire coils are utilized during testing to enhance heat transfer and decrease pressure drop. Heat exchangers, radiators, microchannel sink cooling, solar collectors, solar thermal evaporation, green building, Lithium-ion battery thermal, and other applications are used [14], [54]–[56].

As already reviewed, pressure drop and convection heat transfer behavior from ternary nanofluids in plain tube with wire coil at a constant heat flux have not been investigated much by previous research either experimentally or numerically. In this research, a study was conducted to find out the magnitude of heat transfer performance from Al_2O_3-TiO_2-SiO_2 nanoparticles dispersed into W/EG in plain tube with wire coil, under a constant wall heat flux that was studied experimentally.

2. Methods

2.1. Preparation of Al_2O_3-TiO_2-SiO_2 Ternary Nanofluids

In this present study, three types of nanoparticles are employed, namely Aluminium oxide (Al_2O_3), titanium oxide (TiO_2), and silicon dioxide (SiO_2). Sigma Aldrich (USA) supplied the Al_2O_3 nanoparticles in powder form. At the same time, US Research Nanomaterials, Inc. (USA) supplied the TiO_2 and SiO_2 nanofluids, which are premixed with water. Polychem Indonesia supplied the EG, and distilled water was generated using water distiller equipment. Al_2O_3, TiO_2, and SiO_2 nanoparticles were 13, 50, and 22 nm in size, respectively, with correspondingly purity levels of 99.8%, 99%, and 99.99%. **Table 1** and **Table 2** describe the relevant properties of Al_2O_3, TiO_2, SiO_2, water, and EG in the current investigation.

Table 1. Al_2O_3, TiO_2, and SiO_2 nanoparticle properties [57], [58]

Properties	Unit	Al_2O_3	TiO_2	SiO_2
Density (ρ)	kg m^{-3}	4000	4230	2220
Thermal conductivity (k)	W m^{-1} K^{-1}	40	8.4	1.4
Specific heat (C_p)	J kg^{-1} K^{-1}	773	692	745
Average particle diameter (d)	nm	13	50	22
Molecular mass (M)	g mol^{-1}	101.96	79.86	60.08

Table 2. Ethylene glycol characteristics [59]

Properties	Unit	Ethylene Glycol
Boiling point	°C	195–198
Melting point	°C	-13
Vapour pressure at 20 °C	mmHg	0.08
Density at 25 °C	g ml^{-1}	1.113

A two-step preparation method was used in this investigation to create the ternary nanofluid. The first step in obtaining the predetermined volume of ternary nanofluid is to calculate the volume of each nanofluid. The base fluid was pre-mixed with a 60:40 volume ratio of water and EG. Then, the Al_2O_3-TiO_2-SiO_2 ternary nanofluids were created by combining the base fluid of water/EG with individual Al_2O_3-TiO_2-SiO_2 nanofluids. In addition, all the mono nanofluids were mixed at an optimum composition ratio of 20:16:64 on a scale of 100% by volume to form ternary nanofluids. The optimum value for the acquired hydrodynamic characteristics was used to determine the best composition ratio of the present ternary nanofluids. The infographic process flow in preparation for the Al_2O_3-TiO_2-SiO_2 ternary nanofluid sample is depicted in **Figure 1**.

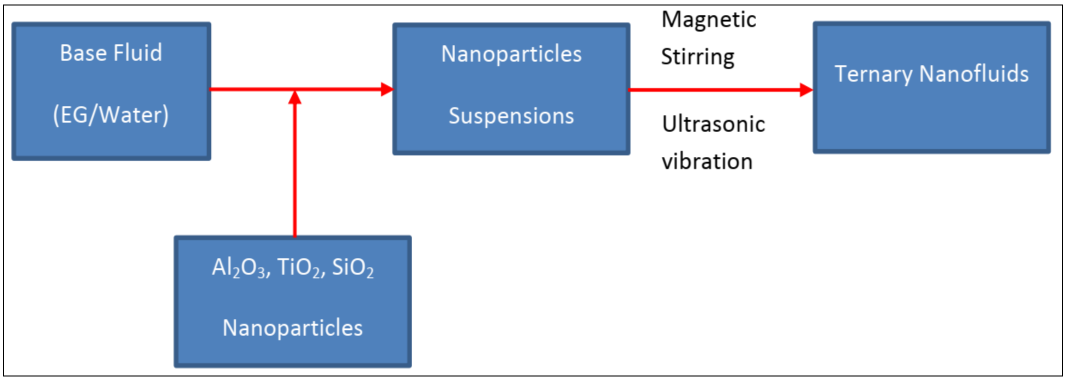

Figure 1. The preparation of ternary nanofluids

This study produced 100 mL total volumes for thermo-physical characteristics of ternary nanofluids, whereas 20 L was used for the forced convection experiment. Various past publications utilized volume concentration units. However, the manufacturer procured the TiO_2 and SiO_2 nanofluids in suspended form, with concentration given in weight percent (wt.%). Eq. (1) is utilized to convert from weight concentration to volume concentration. Further, using Eq. (2), the nanofluids are diluted to a predetermined low-volume concentration. The mono nanofluids are prepared at different volume concentrations of 0.5, 1.0, 1.5, 2.0, 2.5, and 3.0% in the first step.

$$\emptyset = \frac{\omega\rho_{bf}}{\left(1-\frac{\omega}{100}\right)\rho_p + \frac{\omega}{100}\rho_{bf}} \quad (1)$$

$$\Delta V = (V_2 - V_1) = V_1\left(\frac{\emptyset_1}{\emptyset_2} - 1\right) \quad (2)$$

2.2. Measurement of Thermal Conductivity and Dynamic Viscosity

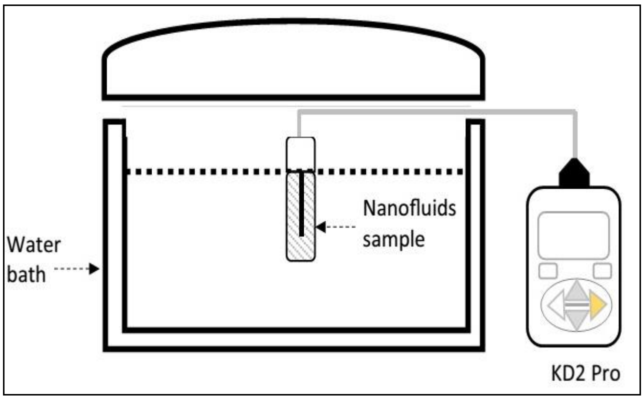

Figure 2. Schematic diagram for thermal conductivity measurement

The thermal conductivity of ternary nanofluids was measured using the KD2 Pro thermal property analyzer by The Decagon Devices, Inc. USA, a widely accepted and accurate instrument in the field of thermal conductivity measurement. As depicted in **Figure 2**, the analyzer consists of a portable controller equipped with a microprocessor, power control, and a sensor for measuring the thermal conductivity of liquid samples. This device can measure thermal properties through a transient line heat source, and it meets IEEE 442-1981 and ASTM D5334 standards. To maintain temperature accuracy between 30 and 70 °C, a Memmert water bath was utilized during the measurement process. Before measuring ternary nanofluids' thermal conductivity, the sensor was validated using glycerine, which the manufacturer provided with a thermal conductivity of 0.285 W/m.K at 25 °C. The sensor measured the thermal conductivity of glycerine at 0.283 W/m.K, with only a 0.7% deviation. This condition demonstrates the reliability and accuracy of the KD2 Pro thermal property analyzer. The study used 40 ml sample containers to hold the ternary nanofluids, and measurements were taken at various temperatures. Later, the sample container was placed in a water bath to maintain a temperature of 30 °C. The KS-1 needle was placed vertically into the sample container and secured with tape to prevent movement during the measurement. At least five measurements were taken for each sample over 15 minutes, and the average values were used for analysis. This method ensures the accuracy and reliability of the thermal conductivity measurements.

This study measured the dynamic viscosity of ternary nanofluids using a Brookfield LVDV-III Rheometer, a specialized instrument designed for viscosity measurements. The instrument has a broad range of viscosity measurements from 1 to 6×10^6 mPa.s. The present study tested the viscosity measurement for the temperature ranges between 30 and 70 °C. The LVDV-III Rheometer operates by regulating the spindle using a calibrated spring essential for its effective operation. The deflection of the calibrated spring is used to calculate the viscous drag of the fluid against the spindle speed, and the deflection is measured using rotating transducers. It is important to note that the torque of the calibrated spring, spindle size, the turn spindle container's form, and rotational speed will significantly affect the viscosity reading. It is recommended that only laminar flow conditions be utilized to measure viscosity percentage torque, which should be between 10 to 100%. The manufacturer states that the viscosity spindle speed may be adjusted between 0.01 to 250 rpm. **Figure 3** depicts the apparatus used for viscosity measurement. Overall, the Brookfield LVDV-III Rheometer is an essential tool for accurately measuring the dynamic viscosity of nanofluids in this study. A 16 ml ternary

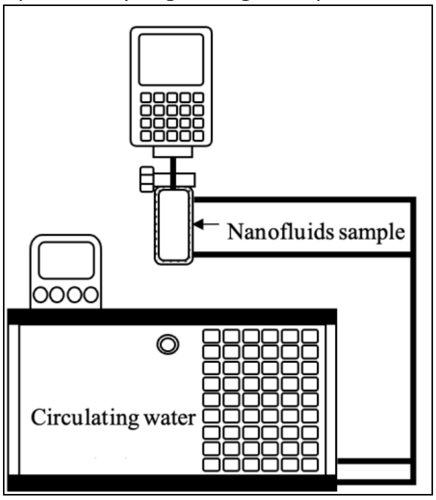

Figure 3. Arrangement of sample ternary nanofluids for dynamic viscosity measurement

nanofluid sample was inserted into a cup inside the cylinder jacket and attached to the rheometer. The water bath was switched on to regulate or maintain the operating temperature. For the goals of this investigation, the dynamic viscosity was evaluated for temperatures from 30 and 70 °C. The temperature of ternary nanofluids was measured using a thermocouple connected to the Rheometer, and the results were displayed on the computer. The RheoCal application was loaded into the computer for data measurement at different torques and temperatures. Every time it switched on the machine, the auto-zero setting was carried out. The spring must be reset to auto-zero for each measurement to minimize error. Thus, the spindle was coupled to the spring to take the measurement. Each sample at different temperatures and concentrations was measured for up to five measurements.

2.3. Force Convection Experimental Setup

In this study, a modified experimental setup based on previous work by Azmi [60] was employed to evaluate forced convection heat transfer. Specifically, a custom experimental system was designed to examine forced convection heat transfer under turbulent flow conditions. The experimental setup used for convective heat transfer in this study is based on the design by Azmi [60], with several improvements and adjustments. The test section, which consists of a copper tube covered with fibreglass and glass wool insulators, was the first component to be developed. The schematic diagram is depicted in **Figure 4**. The setup comprises several components: a thermocouple, pressure transducer, data recorder, flow rate meter, collecting tank, heater regulator, and chiller. Calibration of each component in the test rig is essential to ensure that the settings are precise and suitable for this research. **Table 3** provides a summary of each component of the experimental configuration.

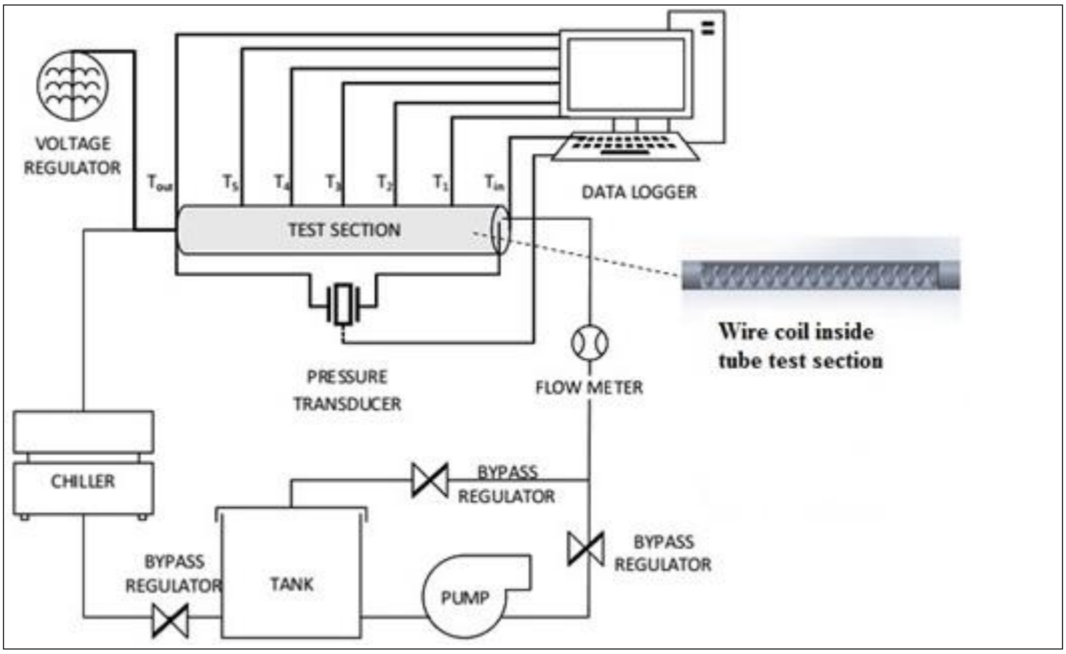

Figure 4. Schematic diagram of forced convection experimental setup

Table 3. Description of components in forced convection setup

Main Section	Description	Function
Test section	Copper tube with D_{in} 16 mm and D_{out} 19 mm, length 1.5 m.	Test section for the heat transfer analysis
Pump	1.0 HP	Distribute working fluid throughout the entire system
Pressure transmitter	Differential type, 2.0 psi	Measure the fluid flow's pressure drop
Bypass regulator	Two units	Control the fluid flow
Data logger	LUTRON BTM-4208SD	Record the experimental data of temperature and pressure
Chiller	2.8 kW	For the cooling process of the system.
Collecting tank	Volume: 0.02 m^3 (20 L)	Store the fluid
Flow rate meter	Range: 0 to 30 LPM	To measure the fluid flow rate
Voltage regulator	2 kW	Supply power for the heating process

2.4. Design of Wire Coil Inserts

To make wire coils, a lathe machine is used to wound a thin, light steel wire with a thickness of 3 mm along a tube with a diameter of 6 mm. This investigation uses wire coil inserts for three pitch-to-diameter ratios, *P/D* of 0.83, 1.50, and 2.50. The consideration of the equalization of heat transfer value and friction factor between pitch ratio (*P/D*) and twist ratio (*H/D*) follows the steps studied by Naik, et al. [61]. A fixed wire coil diameter, *D* = 12 mm, and thickness, *e* = 3 mm, are employed while winding the wire coil pitch on the lathe machine. The parameters of the wire coil and *P/D* selected from the wire coil utilized in this investigation are shown in **Figure 5** and **Table 4**.

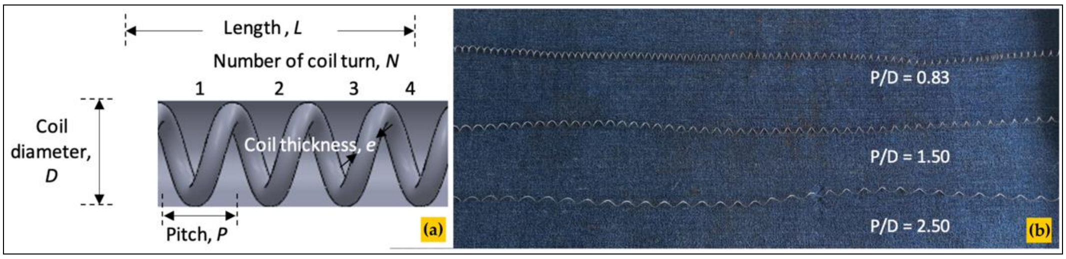

Figure 5. Wire coil inserts design: a) Wire coil characteristics; and b) Wire coil with different pitch ratio (P/D)

Table 4. Characteristic dimensions of the wire coils

Wire coil number	Diameter, *D* (mm)	Thickness, *e* (mm)	Pitch, *P* (mm)	*e/D* (mm/mm)	*P/D* (mm/mm)
WC1	12	3	10	0.25	0.83
WC2	12	3	18	0.25	1.50
WC3	12	3	30	0.25	2.50

2.5. Experiment Procedure

The experimental investigation began by validating the test setup with water: EG (60:40) mixture to investigate forced convection heat transfer. A total of 20 L of water: EG-based fluids were transferred to the collecting tank, and the pump was activated to circulate the fluids flow throughout the system. The bypass valve regulator was used to regulate the flow of fluids in the system ensure proper connections and avoid pipe leaks. Flow rates ranging from 4 to 18 LPM were employed in this investigation. The input power of 750 W was supplied by turning on the voltage regulator on the control screen. To maintain the bulk temperature of the working fluid at 70 °C, a system chiller was used. The thermocouple and differential pressure transducer were connected to the data recording system to record the temperature and pressure drop of the experimental data. The flowmeter, which measures the flow rate of working fluid flows in litres per minute (LPM), was regulated by a regulator. A LUTRON BTM-4208SD data logger was used to record the experimental data to ensure the accuracy and precision of the data.

The first step is to confirm the reliability of the test setup. Initially, the flow rate was set to the maximum in LPM at a constant operating temperature of 70 °C. The flow or bulk temperature is calculated using the average inlet and outlet temperatures at 70 ± 1 °C. Further, the flow rate of working fluids was reduced from a maximum LPM to a minimum. The data logger is set up to record the pressure drop and temperature reading for one minute after the temperature of the data logger and the flow meter has stabilized under steady-state conditions. Then, the experiment was repeated for ternary nanofluids in a plain tube. The Al_2O_3-TiO_2-SiO_2 ternary nanofluids were tested at 70 °C and various volume concentrations of 0.5 to 3.0%. After the completion of forced convection heat transfer of a plain tube, the experiment was repeated for wire coils with ternary nanofluids. The experimental work was undertaken for a wide range of Reynolds numbers from 2,300 to 12,000 at the bulk temperature of 70 °C. Experiments were performed at constant heat flux boundary conditions for flow in plain tubes with wire coil inserts (0.83 ≤ *P/D* ≤ 2.50).

2.6. Heat Transfer Performance

According to Newton's law of cooling, Eq. (3) can express the heat transfer rate to or from a fluid flowing in a tube.

$$Q = h\,A_s(T_s - T_b) \tag{3}$$

where, T_s is the average surface temperature and T_b is the bulk temperature.

The power supply, Q in Watt, is produced by the heater using electrical energy and is expressed by Eq. (4).

$$Q = VI \tag{4}$$

Eq. (5) assumes that there is no heat loss to maintain energy balance and expresses the heat from the tube equal to the heat in fluid flow. The heat supplied to the tube equals the heat in fluid flow.

$$Q = h\,A_s(T_s - T_b) = \dot{m}C_p(T_{outlet} - T_{inlet}) = VI \tag{5}$$

Hence, the heat transfer coefficient and Nusselt number derived are expressed by Eq. (6) and Eq. (7).

$$h_{exp} = \frac{Q}{A_s(T_s - T_b)} \tag{6}$$

$$Nu_{exp} = \frac{h_{exp}\,D}{k} \tag{7}$$

Eq. (8) estimates nanofluids' average heat transfer enhancement in percentage (%).

$$\bar{h}_{enhanced} = \frac{\left[\sum_1^N \frac{h_{nf} - h_{W/EG}}{h_{W/EG}} x100\%\right]}{N} \tag{8}$$

The Reynolds number, Prandtl number, and Nusselt number equations are presented in Eq. (9) to Eq. (11), respectively [62]. The properties of ρ, μ, k and C_p were estimated at bulk temperature, T_b, and obtained from the measurement and mixture relation.

$$Re = \frac{\rho v D}{\mu} \tag{9}$$

$$Pr = \frac{\mu C_p}{k} \tag{10}$$

$$Nu = \frac{hD}{k} \tag{11}$$

In this study, the experimental Darcy friction factor was calculated using Eq. (12), where the pressure drop data from the pressure transducer was utilized. The calculated friction factor was then compared to the theoretical value derived from the Blasius [63] equation to validate the water/EG mixture results. The Blasius [63] equation, shown in Eq. (13), estimates the friction factor for single phase flow in a tube and applies to Reynolds numbers in the range of 3,000 to 5×10^6. The comparison between the experimental and theoretical friction factors is essential to ensure the experimental results' accuracy and the experimental setup's reliability.

$$f_{exp} = \frac{\Delta P_{exp}}{\left(\frac{L}{D}\right)\left(\frac{\rho v^2}{2}\right)} \tag{12}$$

$$f_{Bl} = \frac{0.3164}{Re^{0.25}} \tag{13}$$

D_c is the coil diameter, and D_h is the hydraulic diameter calculated using Eq. (14), as proposed for wire coils in the previous literature [18], [64]. In this study, the pitch ratio symbol is denoted by *P/D* rather than P/D_c.

$$D_h = \frac{D^2 - \pi e^2\,D_c/P}{D + \pi e D_c/P} \tag{14}$$

2.7. Thermal Performance Factor

The thermal performance factor (TPF) equations, as in Eq. (15) are the foundation for the thermal-hydraulic performance analysis, which considers the increase in heat transfer over increasing friction. These parameters allow for the analysis of the effectiveness of ternary nanofluids with inserts made of wire coil. If the modified method improves heat transfer more than the friction factor increment, it is more effective when the TPF value is greater than 1. Therefore, the heat transfer enhancement technique with a higher TPF ratio will perform more efficiently. Subsequently, this section is highlighted the TPF comparison for ternary nanofluids flow in a plain tube, flow with a wire coil. The TPF used in this study also complies with previous literature [47], [65].

Incorporating nanofluids into straight tubes using various inserts can improve heat transfer but may also increase pressure loss. Previous studies have shown that using twisted tape and wire coil inserts enhances the heat transfer performance of nanofluids [19], [66]–[69]. However, the modified system experiences losses due to a higher pressure drop. Therefore, analyzing the hydraulic performance is crucial to determine the effectiveness of the modification approach. Thermal-hydraulic performance, or the thermal performance factor (TPF), measures the increase in heat transfer over friction. It is essential in evaluating the performance of the system.

The TPF is calculated by taking the ratio of Nusselt number to friction factor to the power of 1/3. Using the 1/3 index ensures a fair comparison under the same pumping power, consistent with previous studies [18], [45], [47], [70]. A TPF value greater than one (1) indicates that the heat transfer improvement is greater than the increase in friction factor when using wire coils. The ideal condition is high TPF values for thermal applications, as this indicates that wire coils successfully improve heat transfer with minimal friction factor increase, making them effective [51].

$$TPF(Wire\ Coil) = \frac{\frac{Nu_{nf,WC}}{Nu_{bf,PT}}}{\left(\frac{f_{nf,WC}}{f_{bf,PT}}\right)^{\frac{1}{3}}} \tag{15}$$

2.8. Uncertainty Analysis

The uncertainty analysis results for both instrumentation and physical quantities are summarized in **Table 5** and **Table 6**, respectively. The maximum uncertainty for the instruments used in the experiment was 0.73%, while the maximum uncertainty for the experimental parameters was 0.89%. Overall, the uncertainty analysis provides essential information on the accuracy of the experimental results, and the low uncertainties found in this study suggest that the measurements were precise and reliable.

Table 5. Summary of instruments uncertainty

No	Instruments	Variables	Uncertainty (%)
1	Thermocouple, °C	Bulk temperature, T_b	0.19 – 0.48
2	Thermocouple, °C	Average surface temperature, T_w	0.29 – 0.73
3	Flow meter, LPM	Volume flow rate, $\dot{V}$	0.05 – 0.24
4	Voltage, V	Voltage, V	0.01
5	Current, A	Current, I	0.13
6	Pressure transducer, Psi	Pressure drop, ΔP	0.00014-0.0029

Table 6. Summary of physical quantities uncertainty

No.	Parameters	Uncertainty (%)
1	Reynolds number, Re	0.12 – 0.28
2	Heat flux, q	0.13
3	Heat transfer coefficient, h	0.38 – 0.89
4	Nusselt number, Nu	0.39 – 0.89
5	Friction factor, f	0.13 – 0.36

3. Results and Discussion

3.1. Thermal Conductivity and Dynamic Viscosity of Al_2O_3-TiO_2-SiO_2 Ternary Nanofluids

The enhanced thermal conductivity of the ternary nanofluid is due to the increased volume concentration and temperature. In addition, it is always higher than the water: EG-based mixture. The highest thermal conductivity enhancement of 24.8% was obtained for a volume concentration of 3.0%, as shown in **Figure 6**. Meanwhile, the volume concentration of 0.5% provided the lowest thermal conductivity for 30 °C. The present ternary nanofluid was formulated by the composition ratio of 20:16:64 for three nanoparticle elements of different sizes. The three nanoparticles influenced the effective thermal conductivity of the ternary nanofluid. The diameter of TiO_2 nanoparticles with a size of 50 nm is larger than that of SiO_2 and Al_2O_3 nanoparticles with 22 and 13 nm, respectively. In addition, Al_2O_3 and SiO_2 nanoparticles fill the space gap between the larger TiO_2 nanoparticles to improve the conduction process. Hamid, et al. [71] discussed a similar observation for binary nanofluids. The Brownian motion will result in a higher heat transfer rate during the collision. Increasing the contact area for intermolecular conduction requires a unique and different arrangement of three nanoparticles.

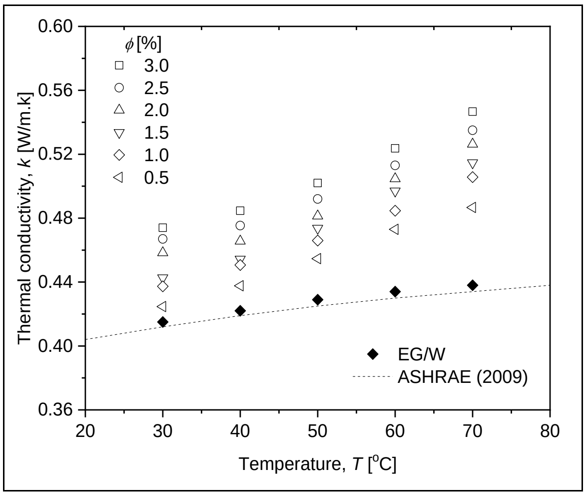

Figure 6. The variation of thermal conductivity for ternary nanofluids at different temperatures and volume concentrations

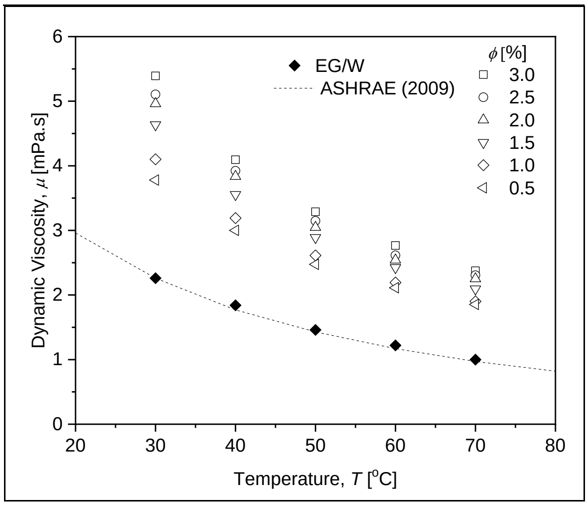

Figure 7. Dynamic viscosity for ternary nanofluids at different temperatures and volume concentrations

Figure 7 presents the dynamic viscosity of ternary nanofluids in the temperature range of 30 to 70 °C for various volume concentrations. The dynamic viscosity of the ternary nanofluids for all volume concentrations follows the based fluid trend, which decreases exponentially with temperature and increases with volume concentration. The 3.0% volume concentration shows the highest value for viscosity at all temperatures. The dynamic viscosity of Al_2O_3-TiO_2-SiO_2 ternary nanofluids is affected by temperature for all volume concentrations, which decreases with temperature and is well agreed with Asadi and Asadi [72].

3.2. Validation of Experimental

Figure 8a and Figure 8a demonstrate the experimental Nusselt number and friction factor data validation for water/EG mixture at a bulk temperature of 70 °C, respectively. The estimation values by the equations of Dittus and Boelter [73] and Blasius [63] confirm the validity of the experimental data arrangement. The figures demonstrate that Dittus and Boelter [73] and Blasius [63] relationship and the experimental value of the water/EG mixture are in good agreement. For Dittus and Boelter [73], the average difference in the Nusselt number between the experimental value and the corresponding estimation is 1.91%. In contrast, 3.52% is the highest deviation for the experimental friction factor compared to the estimation by Blasius [63]. Other researchers also used similar equations by Dittus and Boelter [73] and Blasius [63] as validation standards [43], [57], [74]. The heat transfer coefficient and Nusselt number are higher than the water/EG-based mixture for each wire coil pitch ratio, and they rise with increasing Reynolds number. Additionally, as the wire coil pitch ratio falls, the heat transfer coefficient and Nusselt number rise.

3.3. Heat Transfer Performance with Wire Coil Inserts

Figure 9 show the heat transfer coefficient and Nusselt number, respectively, for flow in a tube with wire coil inserts at different volume concentrations of ternary nanofluids. A pitch ratio of 0.83 led to the most significant heat transfer coefficient increase and complied with all volume concentrations. However, the lowest increase value is shown for the ternary nanofluid with a pitch ratio of 2.50 for each volume concentration. Compared to the water/EG mixture in a plain tube (without coil wire), the heat transfer coefficient increases significantly and rises by more than 100% when the pitch ratio is reduced from 2.50 to 0.83. The 3.0% volume concentration of ternary nanofluid performed with the highest increase in heat transfer and is applicable for all pitch ratios.

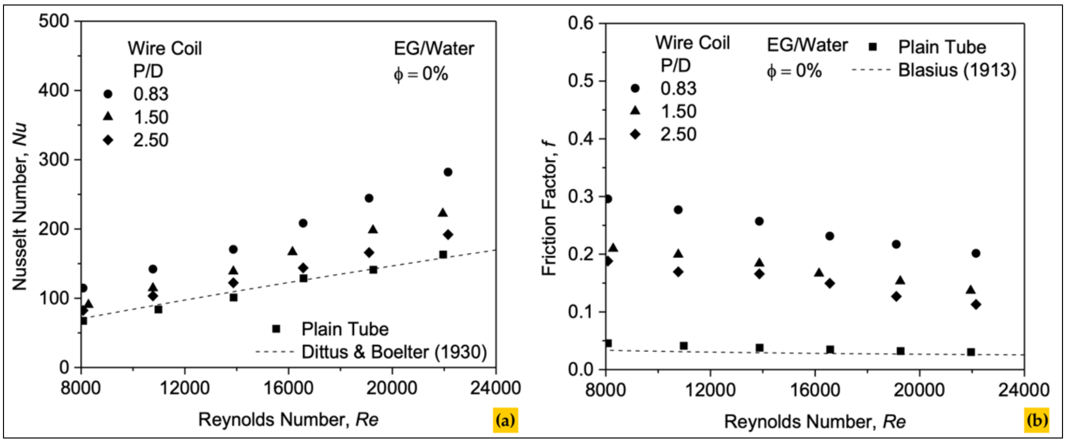

Figure 8. Validation for Nusselt number and friction factor of water/EG mixture with the wire coil:
a) Nusselt Number;
b) Friction factor

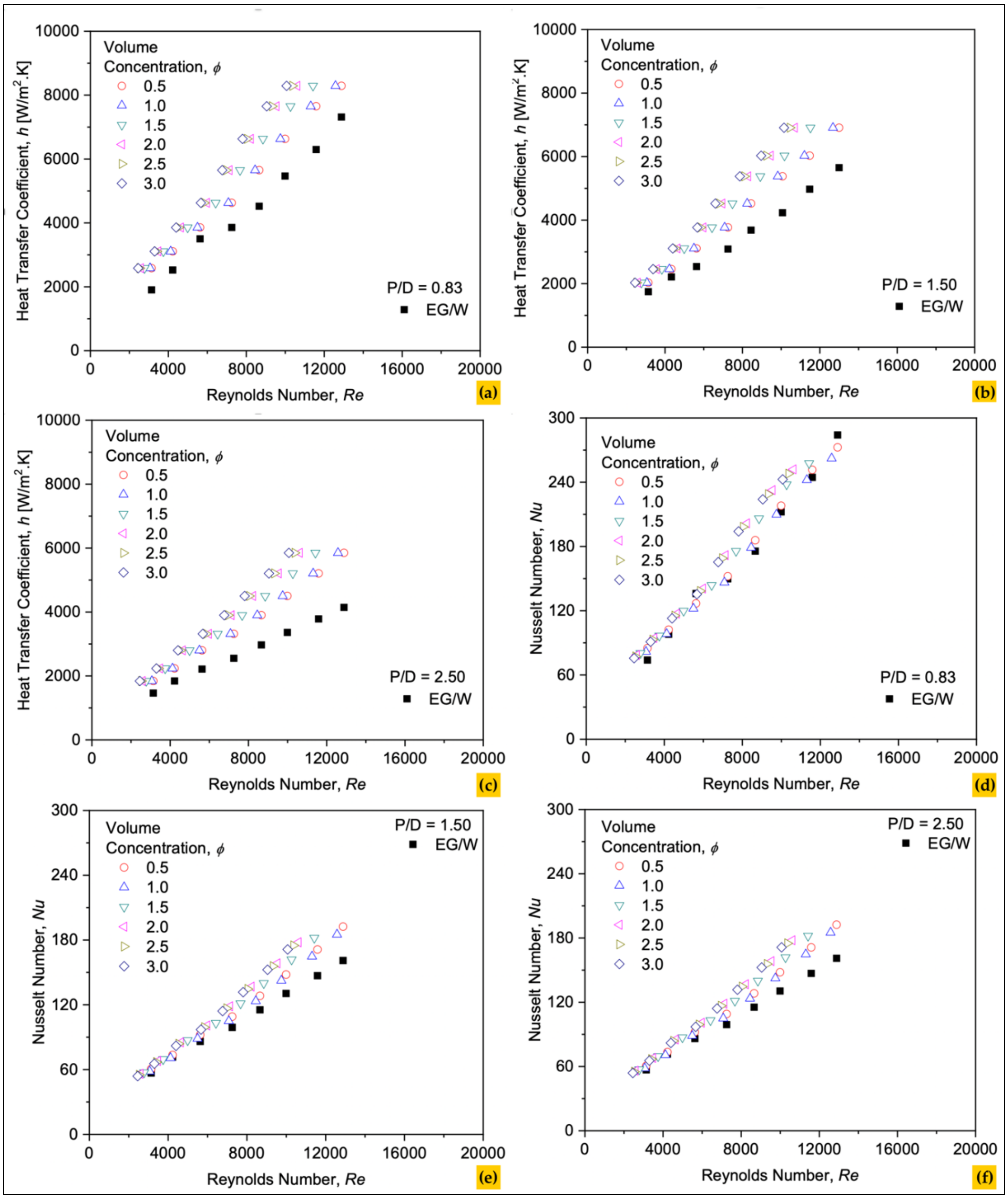

Figure 9. Heat transfer coefficient for ternary nanofluids with the wire coil:
a) P/D = 0.83;
b) P/D = 1.50;
c) P/D = 2.50;
and Nusselt number for ternary nanofluids with the wire coil:
d) wire coil; P/D = 0.83;
e) wire coil; P/D = 1.50;
f) wire coil; P/D = 2.50;

At a pitch ratio of 0.83, the heat transfer enhancement is up to 199.23% higher than the water/EG mixture in a plain tube. The ternary nanofluids at 0.5% volume concentration performed at the lowest heat transfer value than others. The increase in heat transfer coefficient occurs due to the thermal conductivity of ternary nanofluid. Average enhancement in heat transfer coefficient of ternary nanofluids with wire coil for pitch are shown in **Table 7**. The eddy flow created by the wire coil inside the tube causes the liquid to mix. Energy can be transferred more quickly in this state [75]. Furthermore, the mixing flow develops the temperature distribution and increases the steepness of the temperature gradient between the fluid and the wall [70].

Table 7. Average enhancement in heat transfer coefficient of ternary nanofluids with wire coil for pitch ratio of 0.83 ≤P/D ≤ 2.50

Volume concentration, φ (%)	Pitch ratio, *P/D*		
	0.83	1.50	2.50
0.5	114.47	112.45	101.37
1.0	122.77	116.33	104.51
1.5	137.80	126.24	111.77
2.0	145.67	128.37	114.22
2.5	156.02	139.09	117.79
3.0	199.23	152.75	121.90

3.4. Friction Factor with Wire Coil Inserts

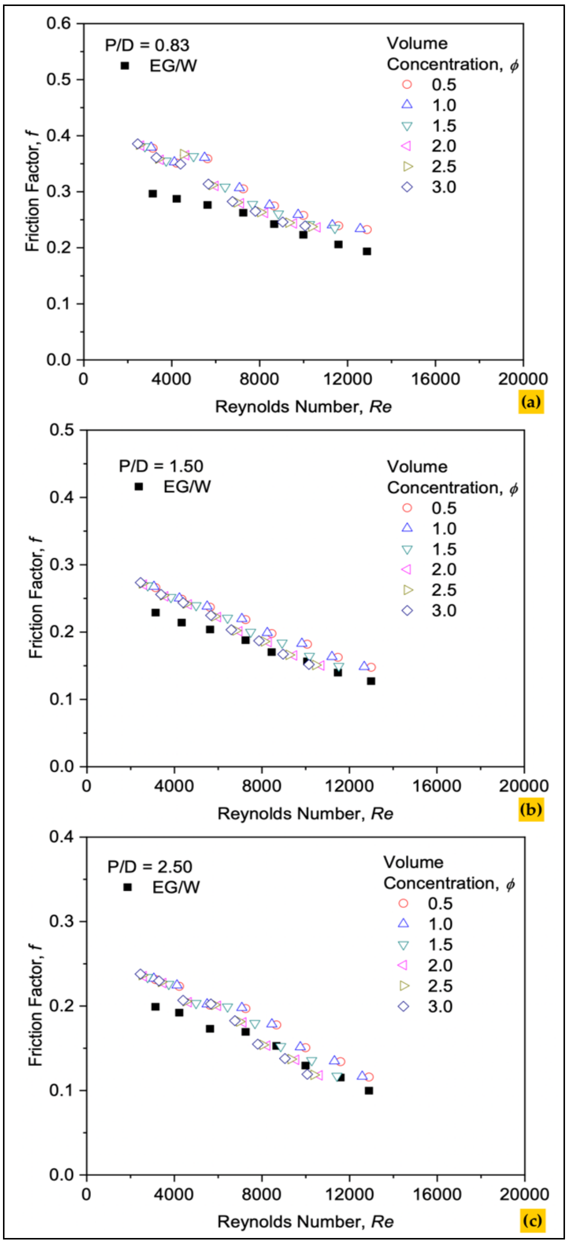

Figure 10. Friction factor of ternary nanofluids with the wire coil : a) P/D = 0.83; b) P/D = 1.50; c) wire coil; P/D = 2.50;

The effect of the volume concentration of ternary nanofluids on the friction factor at different pitch ratios of 0.83 to 2.50 is shown in **Figure 10**. The friction factor decreases with increasing Reynolds number, which follows the trend observed in water/ethylene glycol (EG)-based mixtures. At all volume concentrations and specific wire coils, the friction factors are closely distributed without significant differences. The increase in the friction factor across all volume concentrations is relatively consistent. However, the friction factor decreases as the wire coil's pitch ratio increases. For pitch ratios of 1.50 and 2.50, the average increment of the friction factor for ternary nanofluids was 3.1 and 3.7 times, respectively, compared to the water/EG-based mixture in the plain tube. In contrast, the friction factor at a pitch ratio of 0.83 increased significantly, reaching 5.9 times higher than that of the base fluid in the plain tube. This substantial increase is attributed to fluid dynamic pressure dissipation, as the insertion of wire coils causes high fluid friction. Moreover, a smaller pitch ratio results in a larger surface area due to the increased number of coils. This leads to greater blockage of the coil flow through the flow field, contributing to the higher friction observed. Consequently, the interplay between pitch ratio and friction factor highlights the complex dynamics of fluid behavior in the presence of wire coils [45].

3.5. Thermal Performance Factor

Figure 11 presents the local TPF at a particular Reynolds number with the variation of volume concentration for ternary nanofluids. Like the previous plain tube, the local TPF for the wire coil is also greater than 1.0 and performs higher than that. The local TPF trend occurs similarly by almost

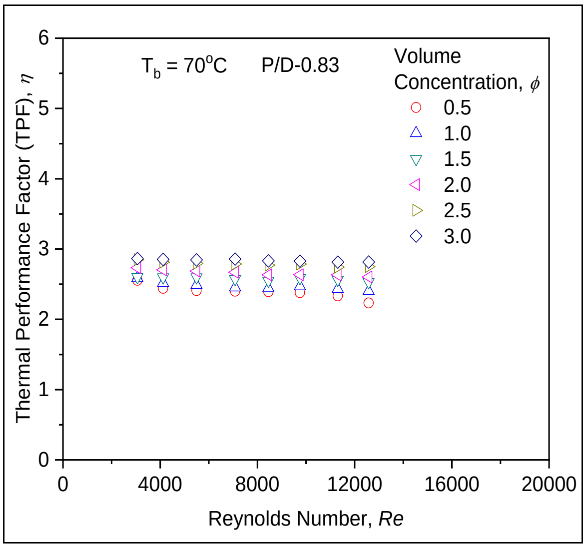

Figure 11. Thermal performance factor for ternary nanofluids with the wire coil

constant with the Reynolds number at a specific volume concentration. In addition, the average TPF increases with volume concentration. The average TPF of the wire coil increases compared to the plain tube and improves further with volume concentrations in the range of 2.39 to 2.84. The minimum and maximum average TPF happened at 0.5 and 3.0% volume concentrations for ternary nanofluids with a wire coil. The average TPF for the wire coil was improved significantly due to enhancement in the Nusselt number is more dominant than the increase in friction factor. Subsequently, the TPF is expected with a higher ratio.

Figure 12 shows the ternary nanofluid's average thermal performance factor at different pitch ratios and volume concentrations. This figure evaluates the pitch ratio's influence on the TPF performance for a wide range of volume concentrations of ternary nanofluids. **Figure 12a** confirms that the TPF at a certain pitch ratio is higher than the plain tube for a particular volume concentration. The TPF increases with a decreasing pitch ratio of more than 2.0 for all volume concentrations and pitch ratios. At a pitch ratio of 0.83, 3.0% volume concentration performs better TPF than other 0.5 to 2.5% volume concentrations.

Meanwhile, **Figure 12b** presents the effect of the TPF on the volume concentration at different pitch ratios. The TPF ratios slightly increase with volume concentration for a particular pitch ratio. The figure shows that the 0.83 pitch ratio performs with the highest TPF ratio and applies to all volume concentrations. The 3.0% volume concentration has the highest TPF compared to the other concentrations. This circumstance occurs because the increase in the Nusselt number is more significant than the friction factor. Therefore, the heat transfer performance dominates the overall system performance.

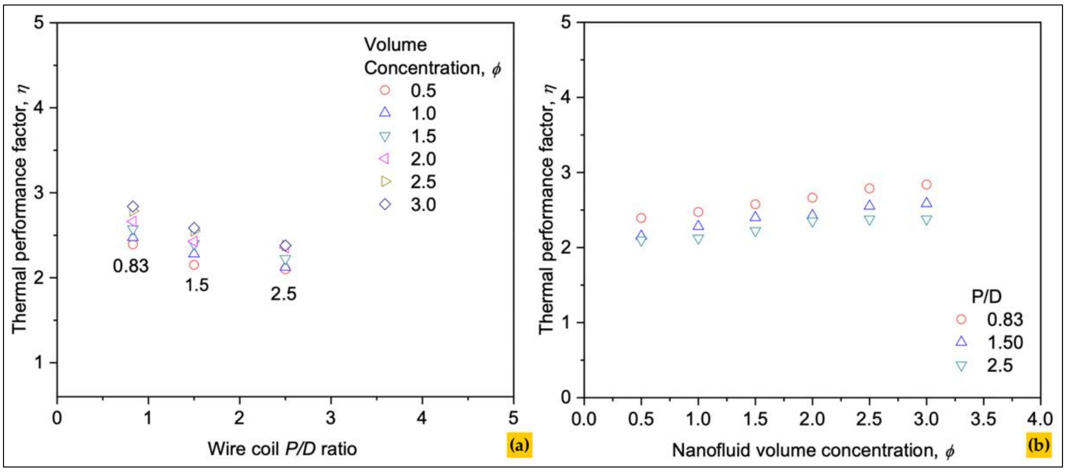

Figure 12. Friction factor of ternary nanofluids with the wire coil : a) P/D = 0.83; b) P/D = 1.50; c) wire coil; P/D = 2.50;

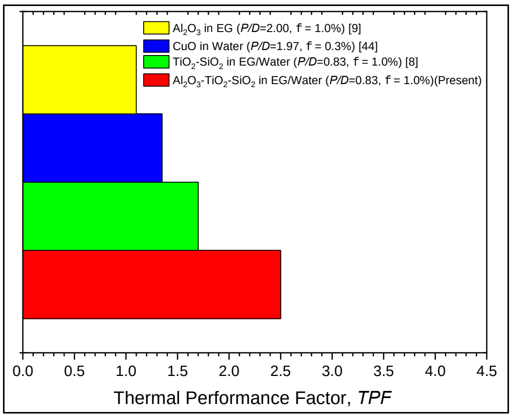

Figure 13. Thermal performance factor for ternary nanofluids with the wire coil

Figure 13 presents to compare the TPF of this research with the TPF available in the literature. Naik et al. [61], Goudarzi and Jamali [19], used air and EG and a single nanofluid as the working fluid in their research. Azmi et al. [18], using TiO_2-SiO_2 nanofluids with EG/Water working fluid. The comparison is considered to be a previous experimental study with a pitch ratio of less than 2.0. From the Figure, there is no data comparable to the data of the current research done. This observation can confirm that the ternary nanofluid flow with wire coils in the tube is suitable for heat exchanger applications.

4. Conclusion

In the present study, highest thermal conductivity enhancement of 24.8% was obtained for ternary nanofluids at 3.0% volume concentration. The 3.0% volume concentration also shows the highest viscosity at all temperatures. Based on experimental, the maximum heat transfer improvement for ternary nanofluids in a plain tube, with wire coil (*P/D*-0.83), was attained by 3.0% volume concentration of up to 199.23%. The average TPF of the wire coil increases compared to the plain tube and improves further with volume concentrations in the range of 2.39 to 2.84. The minimum and maximum average TPF happened at 0.5 and 3.0% volume concentrations for ternary nanofluids with a wire coil.

Acknowledgments

The authors are grateful to the Universiti Malaysia Pahang Al-Sultan Abdullah, Universitas Muhammadiyah Jakarta, and National Research and Innovation Agency of Indonesia for supports and expertise that greatly assisted in the research.

Authors' Declaration

Authors' contributions and responsibilities - The authors made substantial contributions to the conception and design of the study. The authors took responsibility for data analysis, interpretation, and discussion of results. The authors read and approved the final manuscript.

Funding – No funding information from the authors.

Availability of data and materials - All data is available from the authors.

Competing interests - The authors declare no competing interest.

Additional information – No additional information from the authors.

References

[1] S. Junus *et al.*, "Effect of current, time, ethanol concentration, and pH electrolyte on ZnO coated carbon fiber using electrochemical deposition method," *Mechanical Engineering for Society and Industry*, vol. 3, no. 2, pp. 105–113, 2023, doi: 10.31603/mesi.10493.

[2] A. Z. Ziva, Y. K. Suryana, Y. S. Kurniadianti, A. Bayu, D. Nandiyanto, and T. Kurniawan, "Recent Progress on the Production of Aluminum Oxide (Al2O3) Nanoparticles: A Review," *Mechanical Engineering for Society and Industry*, pp. 54–77, 2021, doi: 10.31603/mesi.5493.

[3] S. Pambudi, N. Ilminnafik, S. Junus, and M. N. Kustanto, "Experimental Study on the Effect of Nano Additives γAl2O3 and Equivalence Ratio to Bunsen Flame Characteristic of Biodiesel from Nyamplung (Calophyllum Inophyllum)," *Automotive Experiences*, vol. 4, no. 2, pp. 51–61, 2021, doi: 10.31603/ae.4569.

[4] P. Puspitasari, A. A. Permanasari, A. Warestu, G. P. P. Arifiansyah, D. D. Pramono, and T. Pasang, "Tribology Properties on 5W-30 Synthetic Oil with Surfactant and Nanomaterial Oxide Addition," *Automotive Experiences*, vol. 6, no. 3, pp. 669–686, 2023, doi: 10.31603/ae.10115.

[5] S. Safril, W. H. Azmi, N. N. M. Zawawi, and A. I. Ramadhan, "Tribology Performance of TiO2-SiO2/PVE Nanolubricant at Various Binary Ratios for the Automotive Air-conditioning System," *Automotive Experiences*, vol. 6, no. 3, pp. 485–496, 2023, doi: 10.31603/ae.10255.

[6] S. N. S. Z. Abidin, W. H. Azmi, N. N. M. Zawawi, and A. I. Ramadhan, "Comprehensive Review of Nanoparticles Dispersion Technology for Automotive Surfaces," *Automotive Experiences*, vol. 5, no. 3, pp. 304–327, Jun. 2022, doi: 10.31603/ae.6882.

[7] N. N. M. Zawawi, W. H. Azmi, M. F. Ghazali, and A. I. Ramadhan, "Performance Optimization of Automotive Air-Conditioning System Operating with Al2O3-SiO2/PAG Composite Nanolubricants using Taguchi Method," *Automotive Experiences*, vol. 5, no. 2, pp. 121–136, Mar. 2022, doi: 10.31603/ae.6215.

[8] A. I. Ramadhan, W. H. Azmi, R. Mamat, E. Diniardi, and T. Y. Hendrawati, "Experimental Investigation of Cooling Performance in Automotive Radiator using Al2O3-TiO2-SiO2 Nanofluids," *Automotive Experiences*, vol. 5, no. 1, pp. 28–39, Nov. 2021, doi:

10.31603/ae.6111.

[9] A. Kolakoti, M. Setiyo, D. Novia, A. Husaeni, and A. B. Dani, “Enhancing heat transfer performance of automotive car radiator using camphor nanoparticles : experimental study with bibliometric analysis,” *Teknomekanik*, vol. 6, no. 2, pp. 47–67, 2023, doi: 10.24036/teknomekanik.v6i2.25072.

[10] M. Bahrami, M. Akbari, A. Karimipour, and M. Afrand, “An experimental study on rheological behavior of hybrid nanofluids made of iron and copper oxide in a binary mixture of water and ethylene glycol: Non-Newtonian behavior,” *Experimental Thermal and Fluid Science*, vol. 79, pp. 231–237, Dec. 2016, doi: 10.1016/j.expthermflusci.2016.07.015.

[11] A. Boroomandpour, D. Toghraie, and M. Hashemian, “A comprehensive experimental investigation of thermal conductivity of a ternary hybrid nanofluid containing MWCNTs-titania-zinc oxide/water-ethylene glycol (80:20) as well as binary and mono nanofluids,” *Synthetic Metals*, vol. 268, p. 116501, Oct. 2020, doi: 10.1016/j.synthmet.2020.116501.

[12] J.-Y. Jung, C. Cho, W. H. Lee, and Y. T. Kang, “Thermal conductivity measurement and characterization of binary nanofluids,” *International Journal of Heat and Mass Transfer*, vol. 54, no. 9–10, pp. 1728–1733, Apr. 2011, doi: 10.1016/j.ijheatmasstransfer.2011.01.021.

[13] J. K. Lee, J. Koo, H. Hong, and Y. T. Kang, “The effects of nanoparticles on absorption heat and mass transfer performance in NH3/H2O binary nanofluids,” *International Journal of Refrigeration*, vol. 33, no. 2, pp. 269–275, Mar. 2010, doi: 10.1016/j.ijrefrig.2009.10.004.

[14] J. Zeng and Y. Xuan, “Enhanced solar thermal conversion and thermal conduction of MWCNT-SiO2/Ag binary nanofluids,” *Applied Energy*, vol. 212, pp. 809–819, Feb. 2018, doi: 10.1016/j.apenergy.2017.12.083.

[15] A. I. Ramadhan, W. H. Azmi, R. Mamat, K. A. Hamid, and S. Norsakinah, “Investigation on stability of tri -hybrid nanofluids in water-ethylene glycol mixture,” *IOP Conference Series: Materials Science and Engineering*, vol. 469, p. 012068, Jan. 2019, doi: 10.1088/1757-899X/469/1/012068.

[16] J. Sarkar, P. Ghosh, and A. Adil, “A review on hybrid nanofluids: Recent research, development and applications,” *Renewable and Sustainable Energy Reviews*, vol. 43, pp. 164–177, Mar. 2015, doi: 10.1016/j.rser.2014.11.023.

[17] S. Guo, S. Dong, and E. Wang, “Gold/Platinum Hybrid Nanoparticles Supported on Multiwalled Carbon Nanotube/Silica Coaxial Nanocables: Preparation and Application as Electrocatalysts for Oxygen Reduction,” *The Journal of Physical Chemistry C*, vol. 112, no. 7, pp. 2389–2393, Feb. 2008, doi: 10.1021/jp0772629.

[18] W. H. Azmi, K. Abdul Hamid, A. I. Ramadhan, and A. I. M. Shaiful, “Thermal hydraulic performance for hybrid composition ratio of TiO2–SiO2 nanofluids in a tube with wire coil inserts,” *Case Studies in Thermal Engineering*, vol. 25, p. 100899, Jun. 2021, doi: 10.1016/j.csite.2021.100899.

[19] K. Goudarzi and H. Jamali, “Heat transfer enhancement of Al2O3-EG nanofluid in a car radiator with wire coil inserts,” *Applied Thermal Engineering*, vol. 118, pp. 510–517, May 2017, doi: 10.1016/j.applthermaleng.2017.03.016.

[20] F. Akbaridoust, M. Rakhsha, A. Abbassi, and M. Saffar-Avval, “Experimental and numerical investigation of nanofluid heat transfer in helically coiled tubes at constant wall temperature using dispersion model,” *International Journal of Heat and Mass Transfer*, vol. 58, no. 1–2, pp. 480–491, Mar. 2013, doi: 10.1016/j.ijheatmasstransfer.2012.11.064.

[21] A. I. Ramadhan, W. H. Azmi, R. Mamat, and K. A. Hamid, “Experimental and numerical study of heat transfer and friction factor of plain tube with hybrid nanofluids,” *Case Studies in Thermal Engineering*, vol. 22, p. 100782, Dec. 2020, doi: 10.1016/j.csite.2020.100782.

[22] S. M. Mousavi, F. Esmaeilzadeh, and X. P. Wang, “Effects of temperature and particles volume concentration on the thermophysical properties and the rheological behavior of CuO/MgO/TiO2 aqueous ternary hybrid nanofluid,” *Journal of Thermal Analysis and Calorimetry*, vol. 137, no. 3, pp. 879–901, Aug. 2019, doi: 10.1007/s10973-019-08006-0.

[23] H. Adun, D. Kavaz, and M. Dagbasi, “Review of ternary hybrid nanofluid: Synthesis, stability, thermophysical properties, heat transfer applications, and environmental effects,” *Journal of Cleaner Production*, vol. 328, p. 129525, Dec. 2021, doi: 10.1016/j.jclepro.2021.129525.

[24] S. Kashyap, J. Sarkar, and A. Kumar, “Performance enhancement of regenerative evaporative

cooler by surface alterations and using ternary hybrid nanofluids," *Energy*, vol. 225, p. 120199, Jun. 2021, doi: 10.1016/j.energy.2021.120199.

[25] H. Adun *et al.*, "Synthesis and Application of Ternary Nanofluid for Photovoltaic-Thermal System: Comparative Analysis of Energy and Exergy Performance with Single and Hybrid Nanofluids," *Energies*, vol. 14, no. 15, p. 4434, Jul. 2021, doi: 10.3390/en14154434.

[26] A. Dezfulizadeh, A. Aghaei, A. Hassani Joshaghani, and M. M. Najafizadeh, "Exergy efficiency of a novel heat exchanger under MHD effects filled with water-based Cu–SiO2-MWCNT ternary hybrid nanofluid based on empirical data," *Journal of Thermal Analysis and Calorimetry*, vol. 147, no. 7, pp. 4781–4804, Apr. 2022, doi: 10.1007/s10973-021-10867-3.

[27] V. Kumar and R. R. Sahoo, "4 E's (Energy, Exergy, Economic, Environmental) performance analysis of air heat exchanger equipped with various twisted turbulator inserts utilizing ternary hybrid nanofluids," *Alexandria Engineering Journal*, vol. 61, no. 7, pp. 5033–5050, Jul. 2022, doi: 10.1016/j.aej.2021.09.037.

[28] R. R. Sahoo, "Heat transfer and second law characteristics of radiator with dissimilar shape nanoparticle-based ternary hybrid nanofluid," *Journal of Thermal Analysis and Calorimetry*, vol. 146, no. 2, pp. 827–839, Oct. 2021, doi: 10.1007/s10973-020-10039-9.

[29] L. Kundan and M. B. Darshan, "Performance investigation of a concentric double tube heat exchanger using twisted tape inserts and nanofluid," *Particulate Science and Technology*, pp. 1–18, Jul. 2021, doi: 10.1080/02726351.2021.1946729.

[30] N. A. S. Muzaidi *et al.*, "Heat absorption properties of CuO/TiO2/SiO2 trihybrid nanofluids and its potential future direction towards solar thermal applications," *Arabian Journal of Chemistry*, vol. 14, no. 4, p. 103059, Apr. 2021, doi: 10.1016/j.arabjc.2021.103059.

[31] A. N. Abdalla and A. Shahsavar, "An experimental comparative assessment of the energy and exergy efficacy of a ternary nanofluid-based photovoltaic/thermal system equipped with a sheet-and-serpentine tube collector," *Journal of Cleaner Production*, vol. 395, p. 136460, Apr. 2023, doi: 10.1016/j.jclepro.2023.136460.

[32] A. Dezfulizadeh, A. Aghaei, A. H. Joshaghani, and M. M. Najafizadeh, "An experimental study on dynamic viscosity and thermal conductivity of water-Cu-SiO2-MWCNT ternary hybrid nanofluid and the development of practical correlations," *Powder Technology*, vol. 389, pp. 215–234, Sep. 2021, doi: 10.1016/j.powtec.2021.05.029.

[33] R. R. Sahoo and V. Kumar, "Development of a new correlation to determine the viscosity of ternary hybrid nanofluid," *International Communications in Heat and Mass Transfer*, vol. 111, p. 104451, Feb. 2020, doi: 10.1016/j.icheatmasstransfer.2019.104451.

[34] N. A. Shah, A. Wakif, E. R. El-Zahar, T. Thumma, and S.-J. Yook, "Heat transfers thermodynamic activity of a second-grade ternary nanofluid flow over a vertical plate with Atangana-Baleanu time-fractional integral," *Alexandria Engineering Journal*, vol. 61, no. 12, pp. 10045–10053, Dec. 2022, doi: 10.1016/j.aej.2022.03.048.

[35] H. R. Allahyar, F. Hormozi, and B. ZareNezhad, "Experimental investigation on the thermal performance of a coiled heat exchanger using a new hybrid nanofluid," *Experimental Thermal and Fluid Science*, vol. 76, pp. 324–329, Sep. 2016, doi: 10.1016/j.expthermflusci.2016.03.027.

[36] M. Afrand, D. Toghraie, and B. Ruhani, "Effects of temperature and nanoparticles concentration on rheological behavior of Fe 3 O 4 –Ag/EG hybrid nanofluid: An experimental study," *Experimental Thermal and Fluid Science*, vol. 77, pp. 38–44, Oct. 2016, doi: 10.1016/j.expthermflusci.2016.04.007.

[37] M. Hemmat Esfe *et al.*, "Thermal conductivity of Cu/TiO2–water/EG hybrid nanofluid: Experimental data and modeling using artificial neural network and correlation," *International Communications in Heat and Mass Transfer*, vol. 66, pp. 100–104, Aug. 2015, doi: 10.1016/j.icheatmasstransfer.2015.05.014.

[38] K. A. Hamid, W. H. Azmi, M. F. Nabil, and R. Mamat, "Improved thermal conductivity of TiO 2 –SiO 2 hybrid nanofluid in ethylene glycol and water mixture," *IOP Conference Series: Materials Science and Engineering*, vol. 257, p. 012067, Oct. 2017, doi: 10.1088/1757-899X/257/1/012067.

[39] G. Huminic and A. Huminic, "The heat transfer performances and entropy generation analysis of hybrid nanofluids in a flattened tube," *International Journal of Heat and Mass Transfer*, vol. 119, pp. 813–827, Apr. 2018, doi: 10.1016/j.ijheatmasstransfer.2017.11.155.

[40] M. S. Ahmed and A. M. Elsaid, "Effect of hybrid and single nanofluids on the performance characteristics of chilled water air conditioning system," *Applied Thermal Engineering*, vol. 163, p. 114398, Dec. 2019, doi: 10.1016/j.applthermaleng.2019.114398.

[41] L. S. Sundar, M. K. Singh, and A. C. M. Sousa, "Enhanced heat transfer and friction factor of MWCNT–Fe3O4/water hybrid nanofluids," *International Communications in Heat and Mass Transfer*, vol. 52, pp. 73–83, Mar. 2014, doi: 10.1016/j.icheatmasstransfer.2014.01.012.

[42] T. T. Baby and S. Ramaprabhu, "Experimental investigation of the thermal transport properties of a carbon nanohybrid dispersed nanofluid," *Nanoscale*, vol. 3, no. 5, p. 2208, 2011, doi: 10.1039/c0nr01024c.

[43] O. Keklikcioglu and V. Ozceyhan, "Experimental investigation on heat transfer enhancement in a circular tube with equilateral triangle cross sectioned coiled-wire inserts," *Applied Thermal Engineering*, vol. 131, pp. 686–695, Feb. 2018, doi: 10.1016/j.applthermaleng.2017.12.051.

[44] P. Promvonge, "Thermal augmentation in circular tube with twisted tape and wire coil turbulators," *Energy Conversion and Management*, vol. 49, no. 11, pp. 2949–2955, Nov. 2008, doi: 10.1016/j.enconman.2008.06.022.

[45] M. A. Akhavan-Behabadi, M. Shahidi, and M. R. Aligoodarz, "An experimental study on heat transfer and pressure drop of MWCNT–water nano-fluid inside horizontal coiled wire inserted tube," *International Communications in Heat and Mass Transfer*, vol. 63, pp. 62–72, Apr. 2015, doi: 10.1016/j.icheatmasstransfer.2015.02.013.

[46] A. García, J. P. Solano, P. G. Vicente, and A. Viedma, "Enhancement of laminar and transitional flow heat transfer in tubes by means of wire coil inserts," *International Journal of Heat and Mass Transfer*, vol. 50, no. 15–16, pp. 3176–3189, Jul. 2007, doi: 10.1016/j.ijheatmasstransfer.2007.01.015.

[47] K. Abdul Hamid, W. H. Azmi, R. Mamat, and K. V. Sharma, "Heat transfer performance of TiO2–SiO2 nanofluids in a tube with wire coil inserts," *Applied Thermal Engineering*, vol. 152, pp. 275–286, Apr. 2019, doi: 10.1016/j.applthermaleng.2019.02.083.

[48] P. Promvonge, N. Koolnapadol, M. Pimsarn, and C. Thianpong, "Thermal performance enhancement in a heat exchanger tube fitted with inclined vortex rings," *Applied Thermal Engineering*, vol. 62, no. 1, pp. 285–292, Jan. 2014, doi: 10.1016/j.applthermaleng.2013.09.031.

[49] S. K. Saha, "Thermal and friction characteristics of laminar flow through rectangular and square ducts with transverse ribs and wire coil inserts," *Experimental Thermal and Fluid Science*, vol. 34, no. 1, pp. 63–72, Jan. 2010, doi: 10.1016/j.expthermflusci.2009.09.003.

[50] Z. Feng, X. Luo, F. Guo, H. Li, and J. Zhang, "Numerical investigation on laminar flow and heat transfer in rectangular microchannel heat sink with wire coil inserts," *Applied Thermal Engineering*, vol. 116, pp. 597–609, Apr. 2017, doi: 10.1016/j.applthermaleng.2017.01.091.

[51] S. S. Chougule, V. V. Nirgude, P. D. Gharge, M. Mayank, and S. K. Sahu, "Heat Transfer Enhancements of Low Volume Concentration CNT/Water Nanofluid and Wire Coil Inserts in a Circular Tube," *Energy Procedia*, vol. 90, pp. 552–558, Dec. 2016, doi: 10.1016/j.egypro.2016.11.223.

[52] J. P. Solano, R. Herrero, S. Espín, A. N. Phan, and A. P. Harvey, "Numerical study of the flow pattern and heat transfer enhancement in oscillatory baffled reactors with helical coil inserts," *Chemical Engineering Research and Design*, vol. 90, no. 6, pp. 732–742, Jun. 2012, doi: 10.1016/j.cherd.2012.03.017.

[53] A. García, J. P. Solano, P. G. Vicente, and A. Viedma, "Flow pattern assessment in tubes with wire coil inserts in laminar and transition regimes," *International Journal of Heat and Fluid Flow*, vol. 28, no. 3, pp. 516–525, Jun. 2007, doi: 10.1016/j.ijheatfluidflow.2006.07.001.

[54] S. Rana, H. Zahid, R. Kumar, R. S. Bharj, P. K. S. Rathore, and H. M. Ali, "Lithium-ion battery thermal management system using MWCNT-based nanofluid flowing through parallel distributed channels: An experimental investigation," *Journal of Energy Storage*, vol. 81, p. 110372, Mar. 2024, doi: 10.1016/j.est.2023.110372.

[55] C. Liu *et al.*, "Recent advances of plasmonic nanofluids in solar harvesting and energy storage," *Journal of Energy Storage*, vol. 72, p. 108329, Nov. 2023, doi: 10.1016/j.est.2023.108329.

[56] Yew Wai Loon and Nor Azwadi Che Sidik, "A comprehensive review of recent progress of nanofluid in engineering application: Microchannel heat sink (MCHS)," *Journal of Advanced Research in Applied Sciences and Engineering Technology*, vol. 28, no. 2, pp. 1–25, Oct. 2022, doi: 10.37934/araset.28.2.125.

[57] W. H. Azmi, K. Abdul Hamid, N. A. Usri, R. Mamat, and M. S. Mohamad, "Heat transfer and friction factor of water and ethylene glycol mixture based TiO 2 and Al 2 O 3 nanofluids under turbulent flow," *International Communications in Heat and Mass Transfer*, vol. 76, pp. 24–32, Aug. 2016, doi: 10.1016/j.icheatmasstransfer.2016.05.010.

[58] M. F. Nabil, W. H. Azmi, K. A. Hamid, and R. Mamat, "Heat transfer and friction factor of composite TiO 2 –SiO 2 nanofluids in water-ethylene glycol (60:40) mixture," *IOP Conference Series: Materials Science and Engineering*, vol. 257, p. 012066, Oct. 2017, doi: 10.1088/1757-899X/257/1/012066.

[59] National Institute for Occupational Safety and Health (NIOSH), "Ethylene Glycol: Systemic Agent," *CDC*, 2021. .

[60] W. H. Azmi, "Heat transfer augmentation of water based TiO2 and SiO2 nanofluids in a tube with twisted tape," Universiti Malaysia Pahang, 2015.

[61] M. T. Naik, S. S. Fahad, L. Syam Sundar, and M. K. Singh, "Comparative study on thermal performance of twisted tape and wire coil inserts in turbulent flow using CuO/water nanofluid," *Experimental Thermal and Fluid Science*, vol. 57, pp. 65–76, Sep. 2014, doi: 10.1016/j.expthermflusci.2014.04.006.

[62] Y. Cengel and A. Ghajar, *Heat and Mass Transfer: Fundamentals and Applications*, 4th in SI. New York: Mc Graw Hill, 2011.

[63] H. Blasius, "Das Aehnlichkeitsgesetz bei Reibungsvorgängen in Flüssigkeiten," in *Mitteilungen über Forschungsarbeiten auf dem Gebiete des Ingenieurwesens*, Berlin, Heidelberg: Springer Berlin Heidelberg, 1913, pp. 1–41.

[64] J.-Y. San, W.-C. Huang, and C.-A. Chen, "Experimental investigation on heat transfer and fluid friction correlations for circular tubes with coiled-wire inserts," *International Communications in Heat and Mass Transfer*, vol. 65, pp. 8–14, Jul. 2015, doi: 10.1016/j.icheatmasstransfer.2015.04.008.

[65] L. S. Sundar, M. K. Singh, V. Punnaiah, and A. C. M. Sousa, "Experimental investigation of Al2O3/water nanofluids on the effectiveness of solar flat-plate collectors with and without twisted tape inserts," *Renewable Energy*, vol. 119, pp. 820–833, Apr. 2018, doi: 10.1016/j.renene.2017.10.056.

[66] M. Saeedinia, M. A. Akhavan-Behabadi, and M. Nasr, "Experimental study on heat transfer and pressure drop of nanofluid flow in a horizontal coiled wire inserted tube under constant heat flux," *Experimental Thermal and Fluid Science*, vol. 36, pp. 158–168, Jan. 2012, doi: 10.1016/j.expthermflusci.2011.09.009.

[67] T. Srinivas and A. Venu Vinod, "Heat transfer intensification in a shell and helical coil heat exchanger using water-based nanofluids," *Chemical Engineering and Processing: Process Intensification*, vol. 102, pp. 1–8, Apr. 2016, doi: 10.1016/j.cep.2016.01.005.

[68] S. Eiamsa-ard and K. Kiatkittipong, "Heat transfer enhancement by multiple twisted tape inserts and TiO2/water nanofluid," *Applied Thermal Engineering*, vol. 70, no. 1, pp. 896–924, Sep. 2014, doi: 10.1016/j.applthermaleng.2014.05.062.

[69] P. K. Sarma, T. Subramanyam, P. S. Kishore, V. D. Rao, and S. Kakac, "Laminar convective heat transfer with twisted tape inserts in a tube," *International Journal of Thermal Sciences*, vol. 42, no. 9, pp. 821–828, Sep. 2003, doi: 10.1016/S1290-0729(03)00055-3.

[70] M. Chandrasekar, S. Suresh, and A. Chandra Bose, "Experimental studies on heat transfer and friction factor characteristics of Al2O3/water nanofluid in a circular pipe under laminar flow with wire coil inserts," *Experimental Thermal and Fluid Science*, vol. 34, no. 2, pp. 122–130, Feb. 2010, doi: 10.1016/j.expthermflusci.2009.10.001.

[71] K. A. Hamid, W. H. Azmi, M. F. Nabil, R. Mamat, and K. V. Sharma, "Experimental investigation of thermal conductivity and dynamic viscosity on nanoparticle mixture ratios of TiO2-SiO2 nanofluids," *International Journal of Heat and Mass Transfer*, vol. 116, pp. 1143–1152, Jan. 2018, doi: 10.1016/j.ijheatmasstransfer.2017.09.087.

[72] M. Asadi and A. Asadi, "Dynamic viscosity of MWCNT/ZnO–engine oil hybrid nanofluid: An

experimental investigation and new correlation in different temperatures and solid concentrations," *International Communications in Heat and Mass Transfer*, vol. 76, pp. 41–45, Aug. 2016, doi: 10.1016/j.icheatmasstransfer.2016.05.019.

[73] F. W. Dittus and L. M. K. Boelter, "Heat transfer in automobile radiators of the tubular type," *International Communications in Heat and Mass Transfer*, vol. 12, no. 1, pp. 3–22, Jan. 1985, doi: 10.1016/0735-1933(85)90003-X.

[74] D. K. Agarwal, A. Vaidyanathan, and S. Sunil Kumar, "Investigation on convective heat transfer behaviour of kerosene-Al 2 O 3 nanofluid," *Applied Thermal Engineering*, vol. 84, pp. 64–73, Jun. 2015, doi: 10.1016/j.applthermaleng.2015.03.054.

[75] K. Sharifi, M. Sabeti, M. Rafiei, A. H. Mohammadi, and L. Shirazi, "Computational fluid dynamics (CFD) technique to study the effects of helical wire inserts on heat transfer and pressure drop in a double pipe heat exchanger," *Applied Thermal Engineering*, vol. 128, pp. 898–910, Jan. 2018, doi: 10.1016/j.applthermaleng.2017.08.146.